Multiparametric 3T MR Imaging of Prostate Cancer: Histopathologic Correlation Using Customized MRI-Based Specimen Molds

B. Turkbey[1], H. Mani[2], V. Shah[3,4], M. Bernardo[3,4], A. Rastinehad[5], T. Pohida[6], Y. Pang[7], D. Daar[3], C. Benjamin[5], Y. McKinney[1], J. Shih[8], M. J. Merino[2], P. A. Pinto[5], and P. L. Choyke[1]

[1]Molecular Imaging Program, NCI, NIH, Bethesda, MD, United States, [2]Laboratory of Pathology, NCI, NIH, United States, [3]Molecular Imaging Program, NCI, NIH, United States, [4]Imaging Physics, SAIC Frederick, Inc., NCI-Frederick, [5]Urologic Oncology Branch, NCI, NIH, United States, [6]Division of Computational Bioscience, Center for Information Technology, NIH, United States, [7]Philips Healthcare, United States, [8]Biometric Research Branch, NCI, NIH, United States

INTRODUCTION: Prostate cancer is the most common cancer among American men with 217,730 estimated new cases and 32,050 deaths expected in 2010 (1). Magnetic resonance imaging (MRI) including both anatomical and functional sequences has been shown to be effective in detection and local staging of prostate cancer. However, there are limitations in validating MRI findings even with whole mount histopathology as the "gold standard" since free-hand slicing can easily result in deformation and, off-axis slicing of the prostate resulting in histologic sections that are different from MRI making it difficult to assess the true accuracy of MRI (*2*). Herein, we describe a custom-printed specimen mold that is based on the data extracted from the MRI, which allows sectioning the prostate in the exact plane as the *in vivo* MR slices. The findings of multi-parametric (MP) MRI (T2 weighted [T2W] MRI, apparent diffusion coefficient [ADC] maps of diffusion weighted [DW] MRI, MR spectroscopy, dynamic contrast enhanced [DCE] MRI) were then correlated with resulting registered histopathology slices.

METHODS: This prospective single institution study was approved by the local IRB and was compliant with HIPAA; informed consent was obtained from each patient. The study population included forty-five patients (mean age 60.2 years, range 49-75 years) with a mean PSA level of 6.37ng/mL (range 2.3–23.7ng/mL), who had TRUS guided biopsy proven prostate cancer diagnosis prior to MR imaging (Gleason score ranging from 6 to 9). All patients underwent MP MRI of the prostate on a 3 Tesla scanner (*Achieva, Philips Medical Systems, Best, The Netherlands*) using 16-channel cardiac (*SENSE, Philips Medical Systems, Best, The Netherlands*) and endorectal coils (*BPX-30, Medrad, Pittsburgh, PA, USA*). The MRI protocol included tri-plane T2W TSE MRI, DW MRI, 3D MR spectroscopy, DCE MRI. Following imaging, patient specific MRI based specimen molds were created (3). Following robotic radical prostatectomy, and 2-24 hours fixation, the specimen was sliced in 6mm sections in the mold (*3*). Tumors were mapped prospectively on MP MRI blinded to histopathology results by two experienced radiologists. Histopathology specimens were mapped by location, size and, Gleason score by two pathologists blinded to MRI. The customized mold provided tissues blocks that have one to one correspondence to the *in vivo* MR images. The annotated histology images of each whole mount specimens were stringently correlated with the corresponding MP MR images (Figure 1). Sensitivity, specificity, positive and negative predictive values of MP MRI were calculated in peripheral zone (PZ) and central gland (CG). The effects of lesion size [greatest diameter ≤5 mm vs. >5 mm] and Gleason score [≤7 vs. >7]) on sensitivity of MP MRI: were also evaluated.

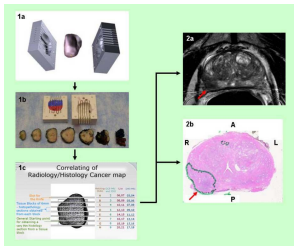

Figure 1: Flow chart for patient-specific MRI based mold creation: (1a), specimen slicing (1b), tissue block and MRI co-registration (1c). 63-year-old male with prostate cancer, axial T2W MRI (2a) and histopathology (2b) confirms the presence of tumor (inked in red with red arrow) (A=anterior, P=posterior, R=right, L=left).

	Sensitivity				Specificity			
	T2W	DCE	MRS	ADC	T2W	DCE	MRS	ADC
Peripheral zone	0.65 (0.04)	0.39 (0.05)	0.17 (0.04)	0.57 (0.04)	0.9 (0.02)	0.97 (0.01)	1 (0)	0.93 (0.02)
Central zone	0.15 (0.08)	0.22 (0.09)	0.08 (0.06)	0.22 (0.09)	1 (0)	0.99 (0)	1 (0)	0.97 (0.01)
Anterior & Central Zone	0.38 (0.07)	0.31 (0.07)	0.15 (0.05)	0.44 (0.07)	0.98 (0.01)	0.99 (0)	1 (0)	0.97 (0.01)
Overall gland	0.58 (0.04)	0.38 (0.05)	0.16 (0.04)	0.53 (0.04)	0.93 (0.01)	0.98 (0.01)	1 (0)	0.95 (0.01)

Table 1

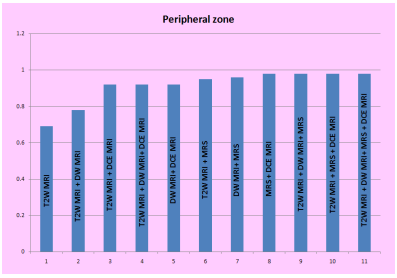

Figure 2

	PPV				NPV			
	T2W	DCE	MRS	ADC	T2W	DCE	MRS	ADC
Peripheral zone (1-4)	0.69 (0.05)	0.86 (0.05)	0.94 (0.04)	0.74 (0.04)	0.89 (0.02)	0.84 (0.02)	0.8 (0.02)	0.87 (0.02)
Central zone (5-6)	0.87 (0.1)	0.86 (0.07)	0.89 (0.1)	0.63 (0.13)	0.92 (0.02)	0.92 (0.02)	0.91 (0.02)	0.92 (0.02)
Anterior & Central Zone	0.73 (0.09)	0.89 (0.04)	0.96 (0.04)	0.75 (0.06)	0.93 (0.01)	0.92 (0.01)	0.91 (0.01)	0.94 (0.01)
Overall gland	0.7 (0.05)	0.86 (0.04)	0.93 (0.04)	0.73 (0.04)	0.9 (0.01)	0.87 (0.01)	0.83 (0.01)	0.89 (0.01)

Table 2

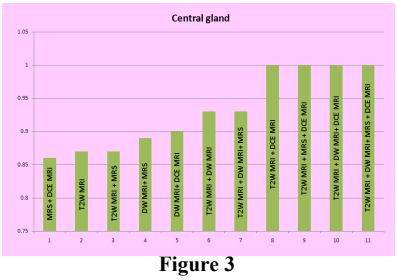

Figure 3

RESULTS: A total of 1746 sectors (1164 in PZ, 582 in CG) were analyzed both in MP MRI and histopathologic specimens. Histopathologic evaluation revealed 341 tumor-positive sectors (280 in PZ, 61 CG). Sensitivity-specificity, PPV-NPV values of MRI sequences in different prostate zones are presented in **tables 1** and **2**, respectively. PPV of MP MRI in PZ and CG are presented in **figures 2** and **3**, respectively. Effects of histopathologic variables (tumor size and Gleason score) on sensitivity of MRI sequences are presented in **tables 3** and **4**, respectively (*standard error values are presented in parenthesis in tables 1-4*).

SENSITIVITY	MRI sequence			
	T2W MRI	DCE MRI	MR spectroscopy	DW MRI
Tumor type				
Grade <=7	0.56 (0.05)	0.30 (0.05)	0.17 (0.04)	0.52 (0.06)
Grade > 7	0.85 (0.05)	0.69 (0.09)	0.30 (0.17)	0.74 (0.08)
Size <= 5mm	0.45 (0.05)	0.15 (0.04)	0.10 (0.04)	0.40 (0.07)
Size > 5 mm	0.75 (0.05)	0.55 (0.07)	0.26 (0.09)	0.68 (0.06)

Table 3 Peripheral zone

SENSITIVITY	MRI sequence			
	T2W MRI	DCE MRI	MR spectroscopy	DW MRI
Tumor type				
Grade <=7	0.47 (0.05)	0.27 (0.05)	0.14 (0.04)	0.45 (0.05)
Grade > 7	0.8 (0.06)	0.69 (0.08)	0.32 (0.14)	0.74 (0.07)
Size <= 5mm	0.37 (0.05)	0.13 (0.03)	0.08 (0.03)	0.33 (0.06)
Size > 5 mm	0.68 (0.05)	0.53 (0.07)	0.25 (0.08)	0.64 (0.06)

Table 4 Overall prostate gland

CONCLUSION: Our data indicates that MP MRI of prostate at 3T enables accurate tumor detection with reasonable sensitivity and specificity values in most cases. ADC maps of DW MRI and DCE MRI were the two most helpful techniques for tumor detection in the central gland, where a significant overlap between tumors and BPH changes usually occurs. MP MRI has better sensitivity for detecting larger (> 5 mm in diameter) and more aggressive (Gleason score of > 7) tumors. The use of the mold enables more exact correlation between each MR parameter and the histopathologic specimen. The customized mold provided tissues blocks that had a one to one correspondence with the *in vivo* MR. It should be noted that this method could be applied to virtually any situation in which a surgical specimen needs to be correlated with a pre-operative MRI. Future work will focus on developing this technique to slice fresh specimens to allow the acquisition of proteomic samples from the tumor to improve assessment of tumor biology and to make thinner slices of 3mm to match the MR images better.

References

1- American Cancer Society. *Cancer Facts & Figures 2010*. Atlanta: American Cancer Society; 2010.
2- Turkbey B, et al. Radiology. 2010;255:89-99.
3- Shah V, et al. Rev Sci Instrum. 2009;80:104301-6.